

Simulation of Laser Beam Propagation With a Paraxial Model in a Tilted Frame

Marie Doumic ^{*} Frédéric Duboc [†] François Golse [‡] Rémi Sentis [§]

December 18, 2007

Abstract

We study the Schrödinger equation which comes from the paraxial approximation of the Helmholtz equation in the case where the direction of propagation is tilted with respect to the boundary of the domain. In a first part, a mathematical analysis is made which leads to an analytical formula of the solution in the simple case where the refraction index and the absorption coefficients are constant. Afterwards, we propose a numerical method for solving the initial problem which uses the previous analytical expression. Numerical results are presented. We also sketch an extension to a time dependant model which is relevant for laser plasma interaction.

1 Introduction

For the simulation of the propagation of a monochromatic laser beam in a medium where the local refractive index is nearby a constant, it is classical to use the paraxial approximation of the Maxwell equations. This approximation takes into account diffraction and refraction phenomena ; it is intensively used for decades in optics and in a lot of models related to laser-plasma interaction in Inertial Confinement Fusion experiments (cf [4],[9], [20], [13] and the bibliography of these references). Let us first recall briefly the outlines of this approximation. Denote by $2\pi\epsilon$ the characteristic wave-length, it is in the order of $1 \mu m$ and is very small compared to the characteristic length of the simulation domain (which is in the order of some mm for the Inertial Confinement plasmas). According to laws of optics, the laser electromagnetic field may be modeled by the solution ψ of the following Helmholtz equation (which comes from the time envelope of the full Maxwell equations):

$$\epsilon^2 \Delta \psi + \psi + 2i\epsilon \nu_t \psi = 0, \tag{1}$$

where we have denoted:

$$\nu_t(\mathbf{x}) = \nu(\mathbf{x}) + i\mu(\mathbf{x}),$$

^{*}Département de Mathématiques et Applications, École Normale Supérieure, projet INRIA BANG, 45 rue d'Ulm, F 75230 Paris cedex 05, France, email: doumic@dma.ens.fr

[†]CEA/Bruyères, B.P.12, 91680 Bruyères-Le-Chatel, France, frederic.duboc@cea.fr

[‡]Ecole Polytechnique, Centre de Mathématiques Laurent Schwartz, 91128 Palaiseau Cedex, France, golse@math.polytechnique.fr

[§]CEA/Bruyères, B.P.12, 91680 Bruyères-Le-Chatel, France, remi.sentis@cea.fr

so ν_t is a complex function, its real part ν corresponds to a conveniently scaled absorption coefficient and its imaginary part μ to the variation of the refractive index ($1 - 2\epsilon\mu$ is equal to the square of the refractive index n up to a multiplicative constant).

We assume also that the light propagates according a fixed direction defined by the unit vector \mathbf{k} . After making the classical WKB expansion:

$$\psi = u \exp\left(\frac{i\mathbf{k}\cdot\mathbf{x}}{\epsilon}\right), \quad (2)$$

equation (1) may read as $2i\nu_t u + 2i\mathbf{k}\cdot\nabla u + \epsilon\Delta_{\perp} u = \epsilon(\mathbf{k}\cdot\nabla)^2 u$, where Δ_{\perp} is the Laplace operator with respect to the transverse variable:

$$\Delta_{\perp}\bullet = \nabla\cdot[(\mathbf{1} - \mathbf{k}\otimes\mathbf{k})\nabla\bullet], \quad \mathbf{1} \text{ being the unit diagonal tensor.}$$

Assuming that u is slowly varying with respect to the longitudinal variable, we can neglect the right hand side of the previous equation. Therefore u satisfies the classical paraxial equation for wave propagation:

$$i\mathbf{k}\cdot\nabla u + \frac{\epsilon}{2}\Delta_{\perp} u + i\nu_t u = 0. \quad (3)$$

For this kind of model, it is usual to handle a simulation box which is a parallelepiped and the laser is assumed to enter into the simulation box on a plane boundary denoted by Γ_0 . Let us denote \mathbf{n} the outward normal vector to the incoming boundary Γ_0 . Classically, the crucial assumption is that the laser beam enters the simulation domain with a very small incidence angle, that is to say the vector \mathbf{k} is almost equal to $-\mathbf{n}$. Then, in such a framework, (3) is a classical linear Schrödinger equation, the operator $\mathbf{k}\cdot\nabla$ plays the part of time derivative and the boundary condition on Γ_0 which reads $u = u^{in}$ (where u^{in} is a given function defined on Γ_0) plays the part of the initial condition. On the other hand, artificial absorbing boundary conditions are to be imposed on the faces of the simulation domain parallel to the vector \mathbf{k} , (see for example [1], [6], [14]). The numerical methods are always implemented on an orthogonal mesh and are based on a splitting with respect to the main spatial variable between the diffraction part ($\frac{\epsilon}{2}\Delta_{\perp} u$) and refraction part ($i\nu_t u$), see [4], [3], [9] for example.

We address in this paper a different case where the incidence angle of \mathbf{k} with $-\mathbf{n}$ is large; these simulations are called tilted frame simulations. This kind of simulations is of particular interest if one has to deal with the crossing between two beams (in the high energy laser devices, a large number of beams are focused on the target, therefore beam crossing may be taken into account, see [7] for a survey on related laser propagation problems); an example of such simulations in a very simplified case may be found on figure 12. This tilted frame model has been considered some years ago by physicists for dealing with beam crossing problems (see [19]).

Simulations in a tilted frame are also necessary for dealing with special situations. For instance for the propagation of a beam in a domain where the profile of the refractive index n is such that $n^2(\mathbf{x}) = n_0^2(1 - \epsilon\mu(\mathbf{x}))$ (with n_0 constant smaller than 1) in a first subdomain \mathcal{D} and $n^2(\mathbf{x}) = \mathcal{N}(\mathbf{x}\cdot\mathbf{n}^*) + \delta\mathcal{N}(\mathbf{x})$ (where $\mathcal{N} \in [0, n_0]$ depends on a one-dimension variable $\mathbf{x}\cdot\mathbf{n}^*$ and $\delta\mathcal{N}$ is small with respect to 1) in a second juxtaposed subdomain \mathcal{D}^H , one must handle the paraxial equation (3) in subdomain \mathcal{D} and the Helmholtz equation (1) in subdomain \mathcal{D}^H . For the numerical solution of (1), one has to solve a huge linear system (corresponding to the discretization of the equation on a very fine grid) and for handling this huge linear system, it is necessary that the variable $\mathbf{x}\cdot\mathbf{n}^*$ corresponds to one of the main direction of \mathcal{D}^H . Therefore the full simulation on $(\mathcal{D} \cup \mathcal{D}^H)$ has to

be performed in a box such that the corresponding normal vector \mathbf{n} must be parallel to \mathbf{n}^* (see [5] for details for this kind of simulations).

In the case of a large incidence angle, the crude expansion $\psi = U \exp(-i\mathbf{n}\cdot\mathbf{x}/\epsilon)$ leads to difficulties and to overcome these difficulties, it has been proposed in [12] to replace the transverse Laplacian by a pseudodifferential operator, but with this approximation, U is not slowly varying with respect to the spatial coordinates therefore it is necessary to handle very fine mesh -at least 10 cells per wave length- to get accurate results. One can also refer to the works in the spirit of [15] in the acoustic framework but the application to the optics problems seems to be difficult.

Here we consider the expansion $\psi = u \exp(i\mathbf{k}\cdot\mathbf{x}/\epsilon)$, with u slowly varying with respect to $\mathbf{k}\cdot\mathbf{x}$, so we have to deal with the tilted frame Laplace operator Δ_{\perp} and one has to supplement the equation (3) with a right incoming boundary condition on Γ_0 . For the statement of this boundary condition, one assumes that a fixed plane wave $\psi^{in} = u^{in} \exp(i\mathbf{k}\cdot\mathbf{x}/\epsilon)$ is coming into the domain where u^{in} is a given function of the variable ranging in Γ_0 . Since for the Helmholtz problem, the boundary condition is classical and may be written as $(\epsilon\mathbf{n}\cdot\nabla + i\mathbf{k}\cdot\mathbf{n})(\psi - u^{in}e^{i\mathbf{k}\cdot\mathbf{x}/\epsilon}) = 0$, then by using (2) and an asymptotic expansion with respect to the small parameter ϵ , the corresponding boundary condition for equation (3) may read in a natural way as:

$$(\epsilon\mathbf{n}\cdot\nabla_{\perp} + 2i\mathbf{k}\cdot\mathbf{n})(u - u^{in}) = 0, \quad (4)$$

where $\nabla_{\perp} = \nabla - \mathbf{k}(\mathbf{k}\cdot\nabla)$ denotes the gradient orthogonal to \mathbf{k} . See [8] for a justification of the paraxial approximation in the special case we are dealing with.

If one sets $\mathbf{x} = (x, y, z)$ in 3D and $\mathbf{x} = (x, y)$ in 2D, the entrance boundary Γ_0 corresponds in this paper to $x = 0$. In the sequel we consider a 2D problem but most of the ideas of this work may be extended to the 3D case.

Equation (3) may be recast as:

$$i(k_x\partial_x u + k_y\partial_y u) + \frac{\epsilon}{2}\Delta_{\perp}u + i\nu_t u = 0,$$

and up to our knowledge, the numerical solution of this kind of equations is novel; the main difficulty is to handle correctly the tilted Laplace operator $\Delta_{\perp}u$. For the mathematical analysis of the problem, one key result is the following (cf. proposition 2). On the half-space $\{(x, y) \text{ s.t. } x \geq 0\}$, if the coefficient ν_t is a positive real constant, after taking the Fourier transform with respect to the y variable, the problem (3)(4) is equivalent to an ordinary differential equation with respect to the x variable and it is possible to exhibit an analytical solution. This analytical formula is the convenient tool for numerical treatment of the diffraction part of (3) in the general case where ν_t is non constant.

The paper is organized as follows. In section 2, after setting classical energy estimates for the problem (3) supplemented by (4), we prove the above mentioned theoretical result. We also give some enlightments on this problem posed in the quadrant $\{(x, y) \text{ s.t. } x \geq 0, y \geq 0\}$, for which we state a transparent boundary condition on $\{y = 0\}$. The section 3 is devoted to the description of the numerical scheme for solving the problem (3) (4) ; it is based on a splitting method with respect to the spatial variable x using fast Fourier transforms on a first step (for the diffraction part) and standard finite difference method on a second step (for the refraction part).

In section 4, we give the numerical results on the initial problem and for a model where the coefficient μ in (3) is replaced by $f(|u|)$ corresponding to the autofocusing which occurs in the laser-plasma interaction (see [18] for instance). From a physical point of view, this term represents a variation of the plasma electronic density caused by the ponderomotive force of the laser. In the last section we consider a more general model where the stationary problem (3) is replaced by

a time dependent one which is coupled to a hydrodynamic system for a suitable modeling of the plasma behavior.

2 Analysis of the Tilted Paraxial Equation

For technical reasons which will appear in the sequel, we assume in this section that

$$\inf_{\mathbf{x}} \nu(\mathbf{x}) > 0. \quad (5)$$

We first study the problem where the simulation domain is the half-space:

$$\mathcal{D} = \{\mathbf{x} = (x, y) \quad \text{s.t.} \quad x > 0\}, \quad \Gamma_0 = \{\mathbf{x} = (0, y)\}.$$

Assuming that μ is a bounded function, we consider the following problem:

$$i\mathbf{k} \cdot \nabla u + \frac{\epsilon}{2} \Delta_{\perp} u - \mu u + i\nu u = 0 \quad \text{on } \mathcal{D}, \quad (6)$$

$$(i\epsilon \mathbf{n} \cdot \nabla_{\perp} - 2\mathbf{k} \cdot \mathbf{n})(u - u^{in}) = 0 \quad \text{on } \Gamma_0. \quad (7)$$

2.1 Energy Estimate

Let us first state the following classical estimate.

Proposition 1 *Let $(i\epsilon \mathbf{n} \cdot \nabla_{\perp} - 2\mathbf{k} \cdot \mathbf{n})u^{in} \in L^2(\mathbb{R})$. If $u \in H^1(\mathcal{D})$ is a solution to the problem (6) (7), it is unique. Moreover, we have the following stability estimate, with a constant C independent of ν, μ :*

$$\iint_{\mathcal{D}} 2\nu |u|^2 + \int_{\Gamma_0} |\mathbf{k} \cdot \mathbf{n}| |u|^2 dy \leq C \int_{\Gamma_0} |(i\epsilon \mathbf{n} \cdot \nabla_{\perp} - 2\mathbf{k} \cdot \mathbf{n})u^{in}|^2 dy.$$

Proof. Let us denote $D = \mathbf{n} \cdot \nabla_{\perp}$. Doing the scalar product of the equation (3) with u and taking its imaginary part, we get:

$$\int_{\Gamma_0} \left(|u|^2 \mathbf{k} \cdot \mathbf{n} + \frac{\epsilon}{2i} (\bar{u} D u - u D \bar{u}) \right) dy + \iint_{\mathcal{D}} 2\nu |u|^2 d\mathbf{x} = 0.$$

According to the boundary condition (7) we check that:

$$\frac{\epsilon}{2i} (\bar{u} D u - u D \bar{u}) = -2\mathbf{k} \cdot \mathbf{n} |u|^2 + \mathcal{I}m(\bar{u}(\epsilon D + 2i\mathbf{k} \cdot \mathbf{n})u^{in}).$$

Then we get:

$$\iint_{\mathcal{D}} 2\nu |u|^2 d\mathbf{x} + \int_{\Gamma_0} |\mathbf{k} \cdot \mathbf{n}| |u|^2 dy = -\mathcal{I}m \left(\int_{\Gamma_0} \bar{u} (\epsilon D + 2i\mathbf{k} \cdot \mathbf{n}) u^{in} dy \right). \quad (8)$$

According to (8), if $(i\epsilon D - 2\mathbf{k} \cdot \mathbf{n})u^{in} = 0$, we see that $\iint_{\mathcal{D}} 2\nu |u|^2 d\mathbf{x} = 0$, so $u = 0$. Therefore we get the uniqueness of the solution of (6) (7).

To obtain the stability inequality, we first see that (8) implies:

$$|\mathbf{k} \cdot \mathbf{n}| \int_{\Gamma_0} |u|^2 \leq \sqrt{\int_{\Gamma_0} |u|^2} \sqrt{\int_{\Gamma_0} |(\epsilon D + 2i\mathbf{k} \cdot \mathbf{n})u^{in}|^2}.$$

Using this estimate, inequality (8) leads to:

$$\iint_{\mathcal{D}} 2\nu |u|^2 d\mathbf{x} + \int_{\Gamma_0} |\mathbf{k} \cdot \mathbf{n}| |u|^2 \leq \sqrt{\int_{\Gamma_0} |u|^2} \sqrt{\int_{\Gamma_0} |(\epsilon D + 2i\mathbf{k} \cdot \mathbf{n})u^{in}|^2} \leq \frac{1}{|\mathbf{k} \cdot \mathbf{n}|} \int_{\Gamma_0} |(\epsilon D + 2i\mathbf{k} \cdot \mathbf{n})u^{in}|^2.$$

◇

By the same technique we get also the following estimate:

$$\iint_{\mathcal{D}} 2\nu |u|^2 + \int_{\Gamma_0} \frac{|\mathbf{k} \cdot \mathbf{n}|}{2} \left| \frac{(i\epsilon D + 2\mathbf{k} \cdot \mathbf{n})u}{2|\mathbf{k} \cdot \mathbf{n}|} \right|^2 = \int_{\Gamma_0} |\mathbf{k} \cdot \mathbf{n}| \left(|u|^2 + \frac{1}{2} \left| \frac{(i\epsilon D - 2\mathbf{k} \cdot \mathbf{n})u^{in}}{2|\mathbf{k} \cdot \mathbf{n}|} \right|^2 \right),$$

which says that the absorbing energy plus the the outgoing energy is equal to the incoming energy.

2.2 Analytical Form of the Solution in the Case ν_t Constant

We now assume that $\mu = 0$ and ν is constant for getting an analytical form of the solution to (3) (4). We denote $\mathbf{k} = (k_x, k_y)$ and g the function defined by:

$$2k_x g = i\epsilon k_y (k_x \partial_y - k_y \partial_x) u^{in} + 2k_x u^{in}. \quad (9)$$

The problem may read as:

$$i(k_x \partial_x + k_y \partial_y)u + \frac{\epsilon}{2} (k_x^2 \partial_{yy}^2 - 2k_x k_y \partial_{xy}^2 + k_y^2 \partial_{xx}^2)u + i\nu u = 0, \quad \text{on } \mathcal{D}, \quad (10)$$

$$i\epsilon k_y (k_x \partial_y - k_y \partial_x)u + 2k_x u = 2k_x g, \quad \text{on } \Gamma_0. \quad (11)$$

In the sequel, the Fourier variables related to x and y respectively are ξ and η . The Fourier transform in x and y are denoted by $\mathcal{F}_x(\bullet)$ and $\mathcal{F}_y(\bullet)$, moreover $\mathcal{F}_y(u; x, \cdot)$ denotes the Fourier transform of $u(x, \cdot)$.

Here and in the sequel, $\sqrt{}$ denotes the principal determination of the square root (its real part is positive). Denote:

$$R_-(i\eta) = i \frac{k_x \eta}{k_y} - i \frac{k_x}{\epsilon k_y^2} \left(1 - \sqrt{1 - 2 \frac{\epsilon k_y \eta}{k_x^2} + 2i\nu \frac{\epsilon k_y^2}{k_x^2}} \right).$$

Since $\nu > 0$, one can define R_- without ambiguity and one checks that $\mathcal{R}e(R_-(i\eta)) < 0$ for all η . Let $\mathcal{S}'(\mathbb{R})$ be the space of tempered distributions.

Proposition 2 *Assume that $g \in \mathcal{S}'(\mathbb{R})$, then there exists a unique distribution $u(x, \cdot)$ continuous from \mathbb{R}^+ into $\mathcal{S}'(\mathbb{R})$, solution to the problem (10)(11). It is given by:*

$$\mathcal{F}_y(u; x, \eta) = \frac{2\mathcal{F}_y(g; \eta)}{1 + \sqrt{1 - 2 \frac{\epsilon k_y \eta}{k_x^2} + 2i\nu \frac{\epsilon k_y^2}{k_x^2}}} e^{R_-(i\eta)x}. \quad (12)$$

It satisfies also:

$$\left(\partial_x - R_-(i\eta) \right) \mathcal{F}_y(u; x, \eta) = 0.$$

Proof of proposition 2

The principle is to take the Fourier transform in y of the problem, and afterwards we shall consider Fourier transform in x of the equation extended to the whole space.

Let u be a solution of the problem (10) (11) and v the extension of u by zero in the whole space: $v(x, y) = u(x, y)\mathbb{1}_{x \geq 0}$. By introducing formally the function v in equation (10) we get:

$$i\mathbf{k} \cdot \nabla v + \frac{\epsilon}{2}\Delta_{\perp}v + i\nu v = \left((ik_x - \frac{\epsilon k_y}{2}(2k_x\partial_y - k_y\partial_x))u(0, y) \right) \delta_{x=0} + \frac{\epsilon k_y^2}{2}u(0, y)\delta'_{x=0}.$$

The term $\partial_x u(0, y)$ is defined by the entrance boundary condition (11), so we get:

$$i\mathbf{k} \cdot \nabla v + \frac{\epsilon}{2}\Delta_{\perp}v + i\nu v = ik_x g(y)\delta_{x=0} - \frac{\epsilon k_y}{2}(k_x\partial_y u(0, y)\delta_{x=0} - k_y u(0, y)\delta'_{x=0}).$$

Assuming that $u \in \mathcal{C}(\mathbb{R}_+, \mathcal{S}'(\mathbb{R}))$, we are allowed to take the Fourier transform of this expression. Let us define $P(X, Y)$ as the polynomial which characterizes the differential operator of the equation, that is to say:

$$P(\partial_x, \partial_y) = i(k_x\partial_x + k_y\partial_y) + \frac{\epsilon}{2}(k_y^2\partial_{xx}^2 - 2k_xk_y\partial_{xy}^2 + k_x^2\partial_{yy}^2) + i\nu.$$

Writing $u_0(y) = u(0, y)$, the Fourier transform in y of the equation in v reads:

$$P(\partial_x, i\eta)\mathcal{F}_y(v; x, \eta) = \frac{\epsilon k_y^2}{2} \left\{ \left(\frac{2ik_x}{\epsilon k_y^2}\mathcal{F}_y(g; \eta) - i\frac{k_x}{k_y}\eta\mathcal{F}_y(u_0; \eta) \right) \delta_{x=0} + \mathcal{F}_y(u_0; \eta)\delta'_{x=0} \right\}.$$

Polynomial P may be factorized as:

$$P(\partial_x, i\eta) = \frac{\epsilon k_y^2}{2} \left(\partial_x - R_+(i\eta) \right) \left(\partial_x - R_-(i\eta) \right), \quad (13)$$

where we define $R_{\pm}(i\eta) = i\frac{k_x}{k_y}\eta - i\frac{k_x}{\epsilon k_y^2} \left(1 \pm \sqrt{1 - 2\frac{\epsilon k_y \eta}{k_x^2} + 2i\nu\frac{\epsilon k_y^2}{k_x^2}} \right)$. Thus:

$$\begin{aligned} & \left(\partial_x - R_+(i\eta) \right) \left(\partial_x - R_-(i\eta) \right) \mathcal{F}_y(v; x, \eta) = \\ & \left(\frac{2ik_x}{\epsilon k_y^2}\mathcal{F}_y(g; \eta) - i\frac{k_x}{k_y}\eta\mathcal{F}_y(u_0; \eta) \right) \delta_{x=0} + \mathcal{F}_y(u_0; \eta)\delta'_{x=0}. \end{aligned} \quad (14)$$

We now show that there is a unique acceptable solution for this ordinary differential equation. Let us take its Fourier transform in x :

$$\left(i\xi - R_+(i\eta) \right) \left(i\xi - R_-(i\eta) \right) \mathcal{F}_x\mathcal{F}_y(v; \xi, \eta) = \frac{2ik_x}{\epsilon k_y^2}\mathcal{F}_y(g; \eta) - i\left(\frac{k_x}{k_y}\eta - \xi\right)\mathcal{F}_y(u_0; \eta).$$

Since $\mathcal{R}e(i\xi - R_{\pm}(i\eta)) \neq 0$, we can divide each side of this equation by $\frac{2}{\epsilon k_y^2}P(i\xi, i\eta)$:

$$\mathcal{F}_x\mathcal{F}_y(v; \xi, \eta) = \frac{\alpha^+(\eta)}{i\xi - R_+(i\eta)} + \frac{\alpha^-(\eta)}{i\xi - R_-(i\eta)},$$

where $\alpha^{\pm}(\eta) = \pm \frac{R_-(i\eta) - i\frac{k_x}{k_y}\eta}{R_+(i\eta) - R_-(i\eta)}\mathcal{F}_y(u_0; \eta) \pm \frac{2ik_x}{\epsilon k_y^2} \frac{1}{R_+(i\eta) - R_-(i\eta)}\mathcal{F}_y(g; \eta)$.

If $\theta \in \mathbb{C} \setminus \mathbb{R}$, one knows that:

$$\frac{1}{i\xi - \theta} = \begin{cases} \mathcal{F}_x(\mathbb{1}_{x \geq 0} e^{\theta x}; \xi) & \text{if } \operatorname{Re}(\theta) < 0 \\ -\mathcal{F}_x(\mathbb{1}_{x \leq 0} e^{\theta x}; \xi) & \text{if } \operatorname{Re}(\theta) > 0 \end{cases}$$

Here $\operatorname{Re}(R_+) = -\operatorname{Re}(R_-) > 0$. According to the previous remark, since $v(x, \cdot) = 0$ for x negative, one gets $\alpha^+(\eta) = 0$ and

$$\mathcal{F}_y(u; x, \eta) = \alpha_{1/2}^-(\eta) e^{R_-(i\eta)x} \mathbb{1}_{x \geq 0},$$

so we get $\mathcal{F}_y(u_0; \eta) = -\frac{2ik_x}{\epsilon k_y^2} \frac{\mathcal{F}_y(g; \eta)}{R_+(i\eta) - i\frac{k_x}{k_y} \eta}$, and the equality (12). The last assertion follows. \diamond

Notice that we can easily calculate, with this formula, the value of the derivative $\mathbf{k} \cdot \nabla u$. As soon as u is regular enough, we can perform an asymptotic expansion in ϵ and ν , and find: $\mathbf{k} \cdot \nabla u = O(\epsilon + \nu)$.

From this result, one deduces the following stability result.

Corollary 1 *If $g \in H^{-\frac{1}{2}}(\mathbb{R})$ then the solution u to (10) (11) is continuous from \mathbb{R}^+ into $L_y^2(\mathbb{R})$, and it satisfies for some constant C not depending on the coefficient ν :*

$$\|u\|_{L_x^\infty(\mathbb{R}_+, L_y^2(\mathbb{R}))} \leq C \|g\|_{H^{-\frac{1}{2}}(\mathbb{R})}.$$

Since C does not depend on the absorption coefficient ν , one can check that if u^{in} is smooth enough, for x fixed, the function $u(x, \cdot)$ converges strongly to a function in L_y^2 when $\nu \rightarrow 0$. Therefore, one may claim that there exists a bounded solution u to (10)(11), even if $\nu = 0$.

Proof.

Let us integrate with respect to η the square modulus of both sides of (12). Since $|e^{R_-(i\eta)x}| = e^{\operatorname{Re}(R_-(i\eta))x} \leq 1$ and:

$$\int |\mathcal{F}_y(g; \eta)|^2 (1 + |\eta|^2)^{-\frac{1}{2}} d\eta = \|g\|_{H^{-\frac{1}{2}}(\mathbb{R})}^2,$$

it suffices to show that there exists a constant $C_1 > 0$ not depending on ν , such that:

$$1 + |\eta|^2 \leq C_1 \left| 1 + \sqrt{1 - \frac{2\epsilon k_y}{k_x^2} \eta + 2i\epsilon\nu \frac{k_y^2}{k_x^2}} \right|^4, \quad \forall \eta \in \mathbb{R}. \quad (15)$$

So, if we denote $X = 1 - \frac{2\epsilon k_y}{k_x^2} \eta$ and $N = 2\epsilon\nu \frac{k_y^2}{k_x^2}$, one first sees that:

$$|1 + \sqrt{X + iN}|^2 = 1 + \sqrt{X^2 + N^2} + 2(X^2 + N^2)^{\frac{1}{4}} \cos\left(\frac{\pi}{4} - \frac{\operatorname{Argtan} X/N}{2}\right) \geq \sqrt{1 + X^2}$$

(indeed the cosine is nonnegative). With $a = \frac{k_x^2}{2\epsilon k_y}$, we have $1 + |\eta|^2 = 1 + a^2(1 - X)^2$ and it is easy to check that $1 + a^2(1 - X)^2 \leq C_1(1 + X^2)$ for $C_1 = 2a^2 + 1$; therefore (15) follows. \diamond

Remark: with the same techniques, one can also find existence and uniqueness of a solution in other spaces, for instance if $\frac{\mathcal{F}_y(g; \eta)}{(1 + |\eta|^2)^{1/8}} \in L_\eta^2(\mathbb{R})$, then we have $u \in L^2(\mathcal{D})$.

Since $|\mathcal{F}_y(g; \eta)| \leq C(1 + |\eta|^2)^{1/2} |\mathcal{F}_y(u^{in}; \eta)|$, that means that if u^{in} is smooth enough (in $H^{3/4}$ for example), then the solution u belongs to $L^2(\mathcal{D})$.

2.3 Remark on the Problem on the Quadrant

We now consider the same problem (10) (11) but restricted to the quadrant $\{(x, y) \text{ s.t. } x \geq 0, y \geq 0\}$. To find a good absorbing boundary condition on the boundary $\{y = 0\}$ (refer to [11]), we formally factorize the differential operator of (10) as follows:

$$P(\partial_x, \partial_y) = \epsilon \frac{k_x^2}{2} (\partial_y - A_+(\partial_x)) (\partial_y - A_-(\partial_x)). \quad (16)$$

where $A_+(\cdot)$ and $A_-(\cdot)$ are the roots of P considered as polynomials in ∂_y :

$$A_{\pm}(\partial_x) = \frac{k_y}{k_x} \partial_x - i \frac{k_y}{\epsilon k_x^2} \left(1 \pm \sqrt{1 + \frac{2i\epsilon k_x}{k_y^2} \partial_x + 2i\epsilon \nu \frac{k_x^2}{k_y^2}} \right) = \frac{k_y}{k_x} \partial_x - i \frac{k_y}{\epsilon k_x^2} \mp \frac{1}{\epsilon k_x^2} \sqrt{-k_y^2 - 2i\epsilon k_x \partial_x - 2i\epsilon \nu k_x^2}.$$

The definition of the fractional derivative is recalled in the appendix. The quadrant problem that we consider consists of (10) (11) supplemented with the boundary condition:

$$\partial_y u - A_+(\partial_x)(u) = 0, \quad \forall x > 0, \text{ for } y = 0. \quad (17)$$

We will see in the appendix how to give a meaning to this boundary condition for $\mathcal{C}_x^b(\mathbb{R}_+, L_y^2(\mathbb{R}_+))$ functions.

Let us define:

$$\hat{K}(\eta) = -\frac{R_-(i\eta) - i \frac{k_x}{k_y} \eta}{R_+(i\eta) - R_-(i\eta)} \quad \text{and} \quad \hat{G}(\eta) = -\frac{2ik_x}{\epsilon k_y^2} \frac{\mathcal{F}_y(g; \eta)}{R_+(i\eta) - R_-(i\eta)}.$$

Then we have the following result whose proof is outlined in the appendix.

Proposition 3 *Assume $g \in H^{-\frac{1}{2}}(\mathbb{R}_+)$ and its support is in $(0, +\infty)$. Let u be the solution of the half-space problem (10) with the incoming boundary condition (11) related to $\tilde{g} = g \mathbf{1}_{y \geq 0}$. Then, there is a unique solution U continuous from \mathbb{R}^+ into $L_y^2(\mathbb{R}_+)$ of (10) (11) (17) and it is given by:*

$$U(x, y) \mathbf{1}_{y \geq 0} = \mathcal{F}_y^{-1} \left(\{ \hat{K}(\eta) \mathcal{F}_y(u_0 \mathbf{1}_{y \geq 0}; \eta) + \hat{G}(\eta) \} e^{R_-(i\eta)x} \right) \mathbf{1}_{y \geq 0}. \quad (18)$$

Moreover:

- i) if $k_y > 0$, then $U = u \mathbf{1}_{y \geq 0}$,
- ii) if $k_y < 0$, and if we take $g(y) = h(y - a)$ with $a > 0$, we get:

$$\lim_{a \rightarrow +\infty} \|U - u \mathbf{1}_{y \geq 0}\|_{L^\infty(\mathbb{R}_+, L_y^2(\mathbb{R}_+))} = 0.$$

3 Numerical Scheme

Let us consider the domain:

$$\mathcal{D} = \{(x, y) : 0 \leq x \leq L_x, y_0 \leq y \leq y_0 + L_y\}.$$

On this domain, we address the numerical solution of the following equation:

$$i(k_x \partial_x + k_y \partial_y)u + \frac{\epsilon}{2} \Delta_{\perp} u + i\nu u - \mu u = 0, \quad (19)$$

where $\nu = \nu(\mathbf{x})$ and $\mu = \mu(\mathbf{x})$; it is supplemented by the same boundary condition as before on $\{x = 0\}$:

$$i\epsilon k_y(k_x \partial_y - k_y \partial_x)u + 2k_x u = 2k_x g,$$

where g is given by (9). It is the same problem as in section 2, except that the coefficients ν and μ may be functions of x . In the sequel, we consider alternatively the case where μ is a function of $|u|$, that is to say:

$$\mu = f(|u|), \quad \text{where } f(w) = e^{-\alpha w^2} - 1,$$

with α a positive constant.

The interesting problems involve a very small coefficient ν , and it may be necessary to have α sufficiently small so that there is no blow-up of the solution.

3.1 Numerical Scheme

Let us set:

$$\nu = \nu_0 + \nu_1, \quad \text{with } \nu_0 = \inf \nu,$$

with ν_0 constant and ν_1 a function of \mathbf{x} .

One discretizes the problem according to a regular grid and we denote by δx , δy the space step in the two directions and by n and j the indices corresponding respectively to the variables x and y : $u_j^n \approx u(n\delta x, j\delta y)$.

The numerical method is based on a space marching technique according to the x variable and a splitting with respect to this variable. According to theorem 2, when the value of u^n is known, it would be possible to evaluate a first intermediate value u^{inter} by solving on $[x^n, x^n + \delta x]$ the following equation:

$$(k_x \partial_x + k_y \partial_y)u - i\frac{\epsilon}{2}\Delta_{\perp} u + \nu_0 u = 0.$$

It would be given by $\mathcal{F}(u^{\text{inter}}) = \mathcal{F}(u^n)e^{R-(i\eta)\delta x}$.

As a matter of fact, in order to have an accurate treatment of the advection term, we prefer to perform the following simple splitting : at each space step $[x^n, x^n + \delta x]$ one solves successively:

$$\begin{aligned} k_x \partial_x u - i\frac{\epsilon}{2}\Delta_{\perp} u + \nu_0 u &= 0, \\ k_x \partial_x u + k_y \partial_y u + (\nu_1 + i\mu)u &= 0. \end{aligned}$$

3.1.1 Initialization

As an initial condition, we take $g = i\epsilon \frac{k_y}{2k_x}(k_x \partial_y - k_y \partial_x)u|_{x=0}^{\text{in}} + u|_{x=0}^{\text{in}}$ where u^{in} is a smooth function of the transverse variable $Y = \mathbf{k}_{\perp} \cdot \mathbf{x} = k_x y - k_y x$ which values zero around the corner points $y = y_0$ and $y = y_0 + L_y$, so one can take its Fourier transform.

To determine the boundary value u^0 of u , we use the formula (12):

$$\mathcal{F}(u^0) = \frac{2\mathcal{F}(g)}{1 + \sqrt{1 - 2\frac{\epsilon k_y \eta}{k_x^2} + 2i\nu|_{x=0}\frac{\epsilon k_y^2}{k_x^2}}}. \quad (20)$$

We obtain $(u_j^0)_j$ by taking the FFT (fast Fourier transform) of g , multiplying it with the discretisation of the function of η expressed above, and then taking the IFFT (inverse fast Fourier transform) of the product.

For classical values of ϵ , *i.e.* for ϵ not too large, the corrective term $i\epsilon k_y(k_x \partial_y - k_y \partial_x)u^{in}$ does not change significantly the result, and it is possible to take simply g equal to u^{in} .

3.1.2 First stage: Fourier transform

The first stage is to solve:

$$k_x \partial_x u - i \frac{\epsilon}{2} \Delta_{\perp} u + \nu_0 u = 0, \quad (21)$$

and we proceed from u^n to $u^{n\#}$. Practically, we get immediately :

$$\mathcal{F}(u^{n\#}) = \mathcal{F}(u^n) e^{(R_-(i\eta) + i\eta \frac{k_y}{k_x}) \delta x}.$$

In fact, we have:

$$R_-(i\eta) + i\eta \frac{k_y}{k_x} = - \frac{2\nu_0}{k_x (1 + \sqrt{1 - 2 \frac{\epsilon k_y \eta}{k_x^2} + 2i\nu \frac{\epsilon k_y^2}{k_x^2}})} - \frac{2i\eta \epsilon (\eta - i\nu_0 k_y)}{k_x^3 (1 + \sqrt{1 - 2 \frac{\epsilon k_y \eta}{k_x^2} + 2i\nu_0 \frac{\epsilon k_y^2}{k_x^2}})^2}. \quad (22)$$

This formula can be used even if ν_0 tends to zero.

So, after a FFT on (u^n) , we multiply it by $e^{(R_-(i\eta) + i\eta \frac{k_y}{k_x}) \delta x}$ and then apply an inverse FFT. We denote $(u_j^{n\#})$ the value of the intermediate function. In order to use the FFT, the values of u^n must coincide on the edges $\{y = 0\}$ and $\{y = L\}$. In fact, we force u^n to be very small in the neighbourhood of these edges (see below); it is the reason why the theoretical results on the quadrant are finally useless here.

3.1.3 Second stage: finite difference scheme

First order scheme.

In this stage, we solve on $[x^n, x^n + \delta x]$ the following equation:

$$k_x \partial_x u + k_y \partial_y u + \nu_1(x) u + i\mu(x) u = 0, \quad (23)$$

or alternatively with μ replaced by $f(|u|)$. To do this, we use standard finite difference methods. Assume that $k_y > 0$ (the case $k_y < 0$ is similar). We consider a non-centered upwind method, given that the CFL stability criteria $\theta \leq 1$ must be checked, where $\theta = \frac{k_y \delta x}{k_x \delta y}$. To avoid difficulties on the edge $\{y = 0\}$ we add to ν_1 an absorbing coefficient, denoted by B , which decreases progressively on the first four meshes and is very large for $\{y = 0\}$. This technique was popularized by [2], and tests show that it cancels a small parasite growth of the solution on the edge. The numerical scheme for this stage is:

$$\frac{k_x}{\delta x} (u_j^{n+1} - u_j^{n\#}) + \frac{k_y}{\delta y} (u_j^{n\#} - u_{j-1}^{n\#}) + \left(\nu_1(x_j^n) + i\mu(x_j^n) \right) \left(\frac{u_{\theta j}^{n\#} + u_j^{n+1}}{2} \right) + B_j^n u_j^{n+1} = 0. \quad (24)$$

For the model with the non linear term $f(|u|)$, the term $\mu(x_j^n)$ is replaced by $f(|u_{\theta j}^{n\#}|)$ where $u_{\theta j}^{n\#} = \theta u_{j-1}^{n\#} + (1 - \theta)u_j^{n\#}$. The point $u_{\theta j}^{n\#}$ represents the point on $\{x = x^n\}$ of the characteristic line passing by (x^{n+1}, y_j) . We initialize the algorithm with $u_{-1}^{n\#} = 0$, what is justified by proposition 3.

Second order scheme.

When $\theta = 1$, the previous scheme gives very accurate results, but in real cases it is not possible to impose this condition, one has $\theta < 1$ and the results are much worse. So we have to improve the numerical scheme when $\theta < 1$ by using a second order scheme as in all advection problems. To do this, we choose a flux-limiter method (see [16]), with the Van Leer function as limiter (tests prove it to be the best one). We introduce the function ϕ which depends on the ratio λ of the gradient of the function $u^\#$ in two neighbouring cells:

$$\phi(\lambda) = \frac{|\lambda| + \lambda}{1 + |\lambda|}.$$

We have to solve simultaneously two scalar equations (one for the real and one for the imaginary part) with the same flux limiter, so we have to choose one single significant quantity to estimate the flux limiter: we choose the energy of the laser, *i.e.* $|u|^2$, and evaluate ϕ in terms of $|u_j|^2$ and not of $|u_j|$:

$$\lambda_j = \frac{|u_j^\#|^2 - |u_{j-1}^\#|^2}{|u_{j+1}^\#|^2 - |u_j^\#|^2}.$$

We now replace, in the first order scheme, the derivative term $u_j^\# - u_{j-1}^\#$ by $F_j - F_{j-1}$ where the flux F_j is defined as:

$$F_j = u_j^\# + \frac{1}{2}(1 - \theta)(u_{j+1}^\# - u_j^\#)\phi(\lambda_j).$$

The second order scheme is now:

$$\frac{k_x}{\delta x}(u_j^{n+1} - u_j^{n\#}) + \frac{k_y}{\delta y}(F_j^n - F_{j-1}^n) + \left(\nu_1(x^n) + i\mu(x_j^n)\right)\left(\frac{u_{\theta j}^{n\#} + u_j^{n+1}}{2}\right) + B_j^n u_j^{n+1} = 0. \quad (25)$$

Remark: Two-Ray Model. One may also consider a more complex model with two rays crossing each other, with two different propagation vectors \mathbf{k}^1 and \mathbf{k}^2 (one with positive and one with negative y -component: $k_y^1 > 0$ and $k_y^2 < 0$.) To do so, it is necessary to evaluate the nonlinear term $f(|u|)$. Theoretically, the laser energy is:

$$|\Psi|^2 = |u^1 e^{i\frac{\mathbf{k}^1 \cdot \mathbf{x}}{\epsilon}} + u^2 e^{i\frac{\mathbf{k}^2 \cdot \mathbf{x}}{\epsilon}}|^2 = |u^1|^2 + |u^2|^2 + 2\mathcal{R}e(u^1 u^{2*} e^{i\frac{(\mathbf{k}^1 - \mathbf{k}^2) \cdot \mathbf{x}}{\epsilon}}).$$

But we are in the framework of W.K.B. approximation and we do not model the fluctuation of the solution at the wavelength level. Hence, the term f has to be taken on a function w corresponding to the variation of the index of refraction, which is here the average value of $|u|$ over a wavelength:

$$w = \sqrt{|u^1|^2 + |u^2|^2}.$$

One considers the following model, for $p = 1, 2$:

$$i\mathbf{k}^p \cdot \nabla w^p + \frac{\epsilon}{2}\Delta_\perp^p + i\nu w^p = f(\sqrt{|u^1|^2 + |u^2|^2})w^p.$$

The first stage of the previous scheme is the same as before : for each ray, we consider the equation (21) with its own propagation direction \mathbf{k}^1 or \mathbf{k}^2 . The interaction between the two rays changes only the nonlinear term of the second stage.

3.2 Properties of the Scheme

Stability

Proposition 4 *The numerical first order scheme is monotone decreasing for the l^2 -norm, i.e the following inequality stands:*

$$\forall n \in \mathbf{N}, \quad \|(u_j^n)_j\|_{l^2} \leq \|(u_j^{n+1})_j\|_{l^2}. \quad (26)$$

Moreover, the previous inequality is strict if $\nu \neq 0$.

Proof.

1. First and second stages: Fast Fourier Transform (FFT)

Let us denote by ζ the discrete variable associated to η . On the one hand, since:

$$u^{n\#} = IFFT \left(e^{(R_-(i\zeta) + i\zeta \frac{k_y}{k_x}) \delta x} FFT(u^n) \right),$$

and since the FFT conserves the l^2 -norm, we have:

$$\|u^{n\#}\|_{l^2} = \|e^{(R_-(i\zeta) + i\zeta \frac{k_y}{k_x}) \delta x} FFT(u^n)\|_{l^2}.$$

On the second hand, the inequality $\mathcal{R}e(R_-(i\zeta)) \leq 0$ implies that:

$$\|e^{(R_-(i\zeta) + i\zeta \frac{k_y}{k_x}) \delta x} U(\zeta)\|_{l^2} \leq \|U(\zeta)\|_{l^2},$$

so we conclude:

$$\|u^{n\#}\|_{l^2} \leq \|u^n\|_{l^2}.$$

2. Third stage: upwind scheme

The relation (24) gives us that:

$$u_j^{n+1} = \frac{\frac{k_x}{\delta_x} u_j^{n\#} - \frac{k_y}{\delta_y} (u_j^{n\#} - u_{j-1}^{n\#}) - \frac{1}{2} (\nu_1 + if(|u_{\theta_j}^{n\#}|)) u_{\theta_j}^{n\#}}{\frac{k_x}{\delta_x} + \frac{1}{2} (\nu_1 + if(|u_{\theta_j}^{n\#}|)) + B_j^n}.$$

Provided that $\frac{k_x}{\delta_x} u_j^{n\#} - \frac{k_y}{\delta_y} (u_j^{n\#} - u_{j-1}^{n\#}) = \frac{k_x}{\delta_x} u_{\theta_j}^{n\#}$, we obtain:

$$u_j^{n+1} = \frac{\frac{k_x}{\delta_x} - \frac{1}{2} (\nu_1 + if(|u_{\theta_j}^{n\#}|))}{\frac{k_x}{\delta_x} + \frac{1}{2} (\nu_1 + if(|u_{\theta_j}^{n\#}|)) + B_j^n} u_{\theta_j}^{n\#}.$$

This leads to $\|u^{n+1}\|_{l^2} \leq \|(u_{\theta_j}^{n\#})_j\|_{l^2}$. By the triangle inequality:

$$\|(u_{\theta_j}^{n\#})_j\|_{l^2} \leq \theta \|(u_{j-1}^{n\#})_j\|_{l^2} + (1 - \theta) \|(u_j^{n\#})_j\|_{l^2} \leq \|u^{n\#}\|_{l^2},$$

which concludes the proof.

◇

In the linear case $f = 0$, the scheme is obviously consistent, so the theorem implies the convergence.

Convergence towards the classical Schrödinger equation

Notice that if $k_y \rightarrow 0$, then the equation (10) (11) reduces to the classical Schrödinger equation:

$$i\partial_x u + \frac{\epsilon}{2}\partial_{yy}^2 u + i\nu u - \mu u = 0, \quad (27)$$

with a very simple boundary condition (notice that $g \rightarrow u^{in}$):

$$u|_{x=0} = u^{in}. \quad (28)$$

Proposition 5 *If $k_y \rightarrow 0$, our numerical scheme reduces to the classical numerical scheme of the Schrödinger problem (27) (28).*

Proof.

1. Initializing

The formula (20) used in the scheme shows that:

$$\lim_{k_y \rightarrow 0} \mathcal{F}(u; x = 0) = \mathcal{F}(g),$$

so the boundary condition tends to $u|_{x=0} = g$, which is (28).

2. First stage

If k_y tends to zero, *i.e.* when the ray tends to be perpendicular to the boundary, the formula (22) shows that:

$$\lim_{k_y \rightarrow 0} R_-(i\eta) + i\eta \frac{k_y}{k_x} = -\nu_0 - i\frac{\epsilon}{2}\eta^2,$$

so $u^{n\#}$ given by the first stage is the solution of the classical Schrödinger equation:

$$i\partial_x u + \frac{\epsilon}{2}\partial_{yy}^2 u + i\nu_0 u = 0,$$

which is the limit of the advection-Schrödinger equation.

3. Second stage

It corresponds to a classical discretization of the ordinary differential equation:

$$\partial_x u + \nu_1 u + i\mu u = 0.$$

In other words, the scheme is a classical splitting between the dispersion term and the refraction term in the Schrödinger equation (27).

◇

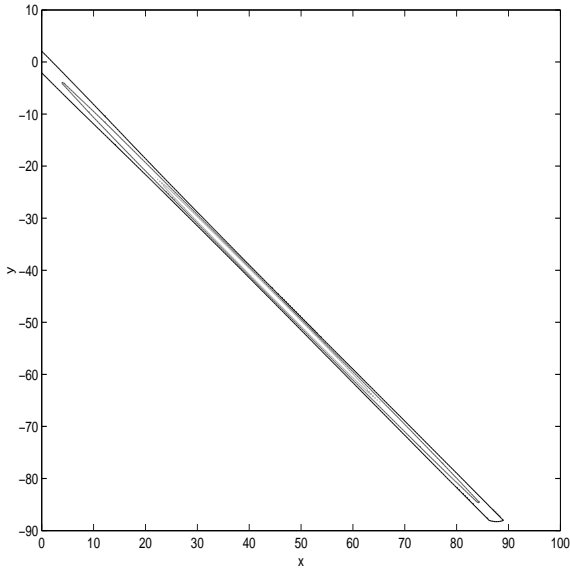


Figure 1: Reference: $\delta_y = 0.4$, $CFL = 1$.
 $L_{foc} = 60.0$, $Max(|u|^2) = 2.14$.

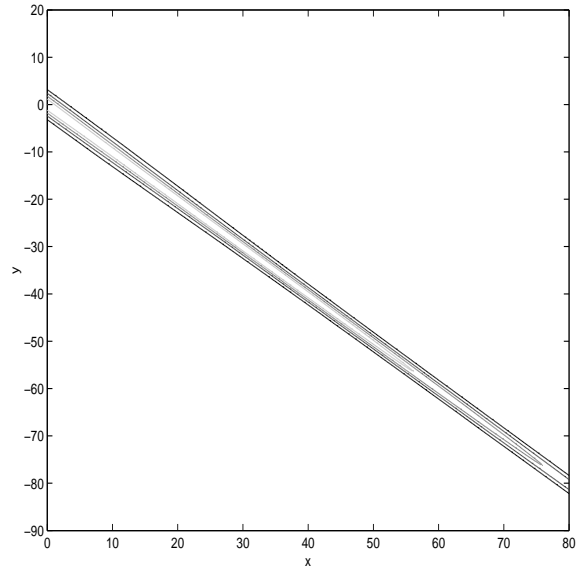


Figure 2: 1st order scheme with $CFL = 0.7$,
 $\delta_y = 0.2$. No focusing observed.

3.3 Numerical Results

Here we give the standard numerical values used in the following results.

1. $L = 2.5 \mu m$: it is approximately the half-width of a speckle of a typical laser beam. For an initial condition, we take a Gaussian $u^{in} = exp(-(\frac{\mathbf{k} \cdot (\mathbf{x} - \mathbf{x}_0)}{L})^2)$. In order to simplify the comparison between different angles of incidence for a same beam, we always take the maximum point of u^{in} be the point $(0, 0)$, *i.e.* $Y_0 = 0$. For the cases with only one ray, we take $\mathbf{k} = (-\frac{\sqrt{2}}{2}, \frac{\sqrt{2}}{2})$: the ray enters in the domain with an angle of -45° .
2. $\epsilon = 0.05 \mu m$, the wavelength of the laser is $2\pi\epsilon \approx 0.3 \mu m$.
3. $\nu_0 = \nu_1 = 5 \cdot 10^{-3} \mu m^{-1}$. The fact that $\nu \approx 1/100 \mu m^{-1}$ means that the laser energy is reduced by a factor $1/e^2$ on a distance of $100 \mu m$. It is also possible to take much smaller absorption values and obtain quite as good results: in other words the absorption does not influence the convergence of the scheme.
4. We take $\alpha = 5 \cdot 10^{-2}$. It depends on the electronic density of the plasma: in the vacuum α would be null. This size order corresponds either to a dense plasma or to a high laser intensity - since we have taken a normalized u^{in} of intensity equal to 1.

All our figures represent $|u|^2$, which is more significant than $|u|$ since it is the energy. To be easier to read, our examples are variations around the case of an incidence angle of 45° , with the previous orders of magnitude and CFL number equal to 1 (see figure 1). With these assumptions, the scheme converges very well as the discretization step decreases.

Convergence of the scheme

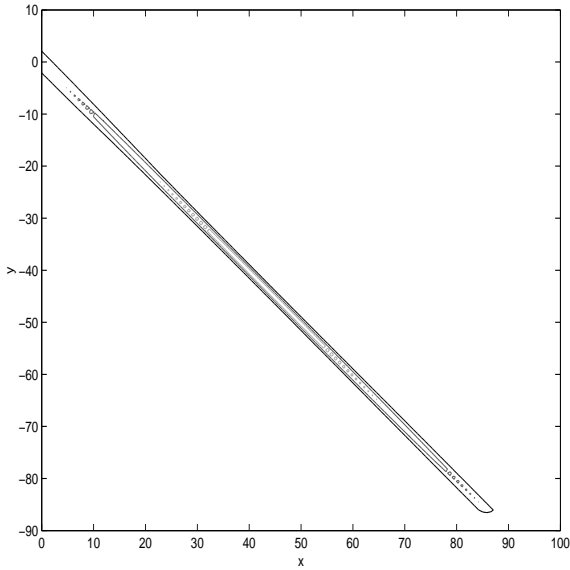


Figure 3: First order, $CFL = 1$. $\delta_x = \delta_y = 0.8$, $L_{foc} = 61.5$ and $Max(|u|^2) = 2.16$.

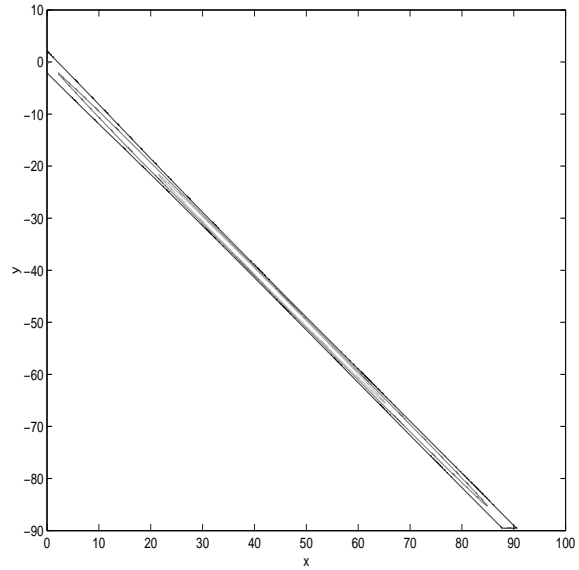


Figure 4: First order, $CFL = 1$. $\delta_x = \delta_y = 0.1$, $L_{foc} = 59.4$ and $Max(|u|^2) = 2.14$.

We take $\epsilon = 0.05$, $\nu_0 = \nu_1 = 0.0005$, $\alpha = 0.05$, and u^{in} a Gaussian of amplitude 1. Due to the α coefficient, focusing occurs: the beam focuses and reaches a maximum, then decreases, and may even focus several times.

Convergence of the first order scheme

If the CFL number is strictly larger than 1, the computed solution blows up, and if $CFL < 1$, the precision quickly vanishes, and the focusing disappears: see figure 2.

We now take the CFL number equal to 1. To verify the convergence of the scheme, we look in each case at the focusing maximal point and check whether its distance L_{foc} to the origin of the ray and its maximal value converge. The conclusion is that we reach an accurate result even for $\delta_x = \delta_y = 0.8$: see figures 3 and 4, to be compared to figure 1. The focusing distance L_{foc} lies between 59.4 and 61.5, and the maximum between 2.14 and 2.16, which gives an error less than 3 percents.

Convergence of the second order scheme

After having tested different functions for the flux limiter, which we always apply at $|u|^2$ and not at the real or imaginary part of the solution, it appears that the Van Leer flux function is the one which gives the most accurate results. With $CFL = 0.4$, we obviously need more points than for $CFL = 1$ but manage anyway, with 2^{10} points (that is, with $\delta_y = 0.1$), in finding a correct approximation: see figures 5 and 6, to be compared to the reference figure 1.

Variation of several parameters

Variation of the incidence angle

To test whether the scheme is accurate for various angles, we make it vary from 5° to 60° (in fact it works also for smaller up to 1° , and bigger up to 80° angles, but this does not have much

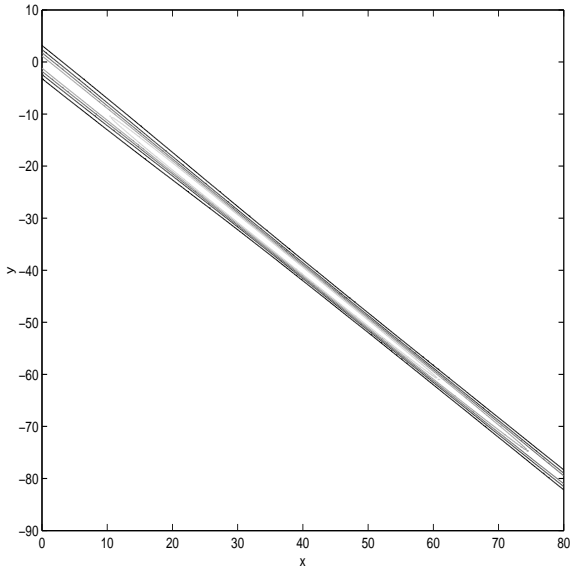


Figure 5: 2nd order, low precision:
 $\delta_x = 0.16$ and $\delta_y = 0.4$.
 $L_{foc} = 50.7$ and $Max(|u|^2) = 1.24$.

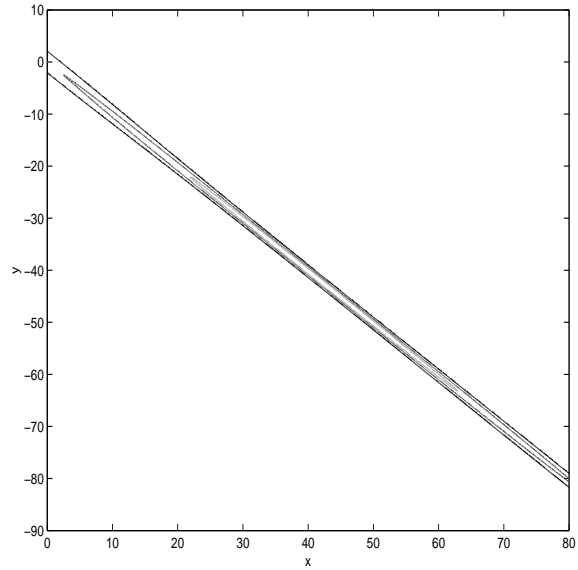


Figure 6: 2nd order, high precision:
 $\delta_x = 0.04$ and $\delta_y = 0.1$.
 $L_{foc} = 60.5$ and $Max(|u|^2) = 2.06$.

practical interest), all the other parameters being constant: see figures 7 to 10, for each of which the convergence of the scheme is very good (we have taken 2^9 points in each direction). We conclude that the focusing distance and the maximum of energy are very well captured: the error is smaller than 5 percents. Hence, our method is valid whatever the angle may be.

Other parameters

- **Variation of ϵ :** the diffusion grows with ϵ . We cannot take it too big: the bigger it is, the larger domain must be in order to obtain a converging solution. In addition, the case $\epsilon = 0$ is outside the scope of this work.

- **Variation of ν_0 and ν_1 :** the scheme can also be used with no absorption, the solution still converges if the other parameters are convenient. The repartition of ν_0 and ν_1 changes the solution by less than 2%, and furthermore only at the end of the domain and without changing the shape of the solution.

- **Variation of α :** for a limit value of α , focusing appears: in our reference case, the limit is for $\alpha = 0.02$. When it is large enough, several focusing points appear, at regular distance from each other: see figure 11, where we have taken the reference case with no absorption. This phenomenon depends of course also of the absorption $\nu_0 + \nu_1$. If α becomes larger, there is a filamentation phenomenon, along with multiple focusing points. In figure 12, we see two rays crossing in the vacuum, *i.e.* $\alpha = 0$.

4 Extension to a Time-Dependent Interaction Model

We now address a model where a tilted paraxial equation equation is coupled with a hydrodynamic model in order to study filamentation and possibly deflexion due to a transverse flow. Under the hypothesis of a small incidence angle, this model has been extensively used by physicists for a long time and it is also addressed in [4],[3],[9] for example and the references therein (for a derivation of

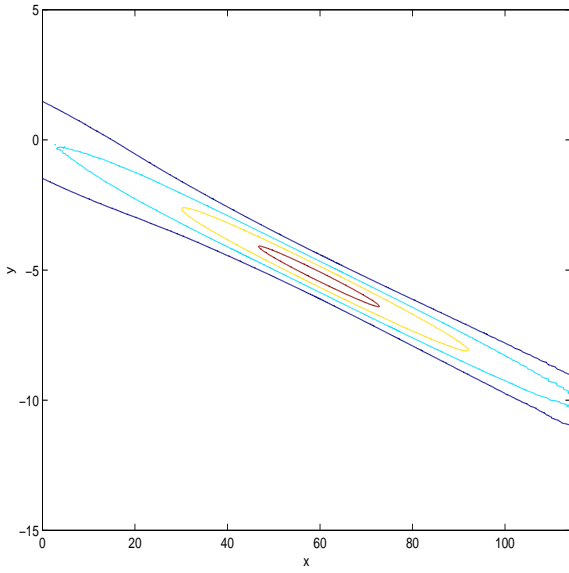


Figure 7: Incidence angle 5° , $CFL = 1$.
 $L_{foc} = 60.6$ and $Max(|u|^2) = 2.2$.

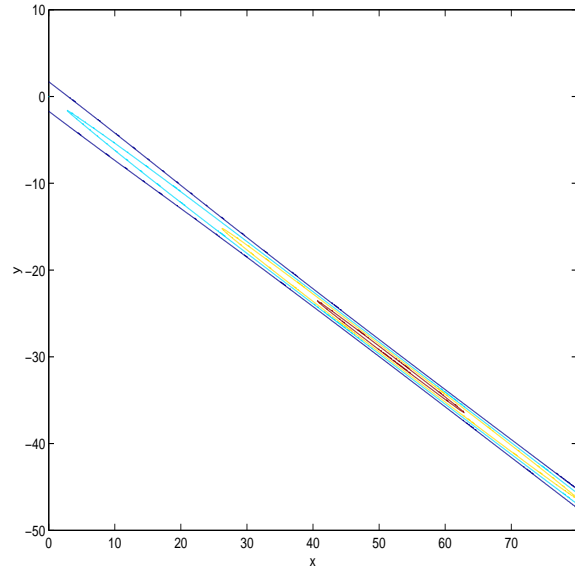


Figure 8: Incidence angle 30° , $CFL = 1$.
 $L_{foc} = 59.4$ and $Max(|u|^2) = 2.2$.

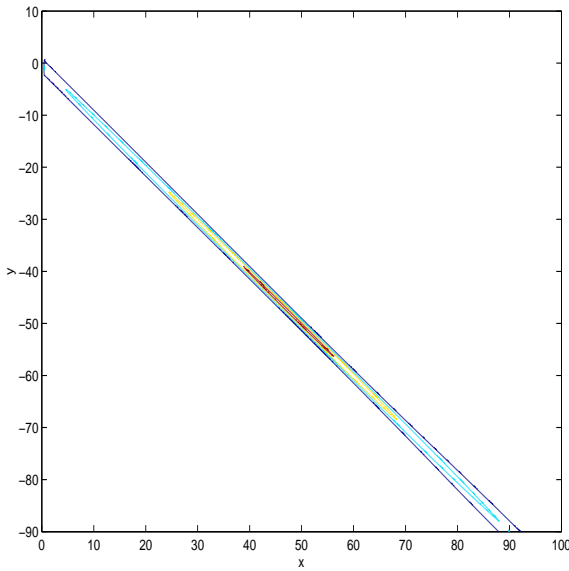


Figure 9: Incidence angle 45° , $CFL = 1$.
 $L_{foc} = 59.8$ and $Max(|u|^2) = 2.14$.

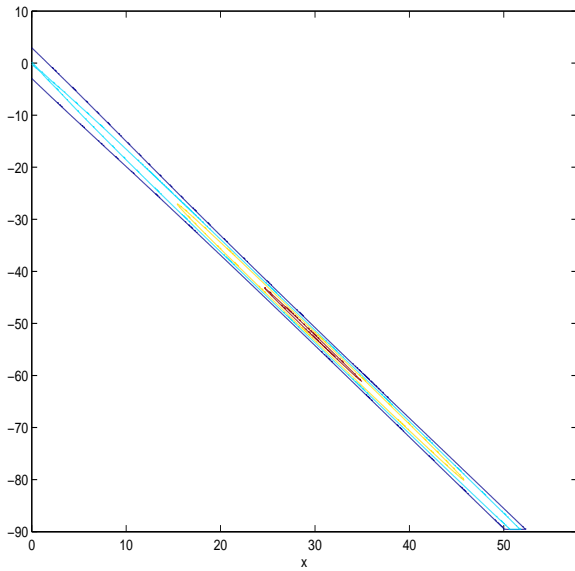


Figure 10: Incidence angle 60° , $CFL = 1$.
 $L_{foc} = 59.7$ and $Max(|u|^2) = 2.10$.

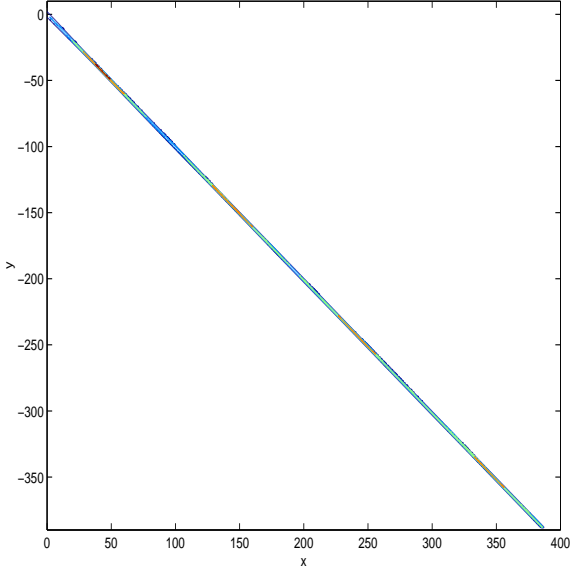


Figure 11: Multiple and regular focusing observed for $\alpha = 0.05$, $\nu_0 = \nu_1 = 0$, standard hypothesis.

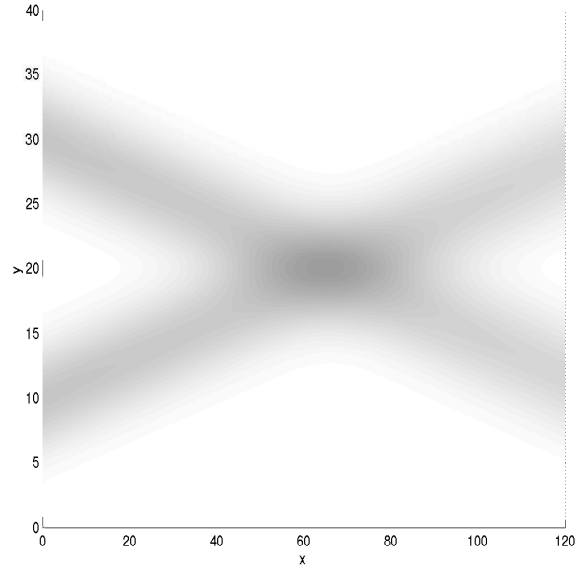


Figure 12: 2 beams crossing with $\alpha = 0$ (vacuum).

this model, see [17] for example).

4.1 The Model and the Numerical Method

Modeling of the plasma.

By taking the critical density (depending only on the laser wave length) as a reference density, one defines a non-dimension electron density $N = N(t, \mathbf{x})$; so the the plasma may be characterized only by this quantity, the plasma velocity $\mathbf{U} = \mathbf{U}(t, \mathbf{x})$ and the electron density $T_e(t, \mathbf{x})$.

Then, the simplest model is the following one. The pressure $P = P(N, T_e)$ is assumed to be a smooth function of the density N and of the electron temperature T_e (which is assumed to be a very smooth fixed function of the position \mathbf{x}), for example $P(N, T_e)$ may be the sum of two terms equal to N^3 and NT_e up to multiplicative constants. Then one considers the following barotropic Euler system:

$$\frac{\partial}{\partial t} N + \nabla(N\mathbf{U}) = 0, \quad (29)$$

$$\frac{\partial}{\partial t}(N\mathbf{U}) + \nabla(N\mathbf{U}\mathbf{U}) + \nabla(P(N, T_e)) = -N\gamma_p \nabla|\Psi|^2. \quad (30)$$

The term $\gamma_p \nabla|\psi|^2$ corresponds to a ponderomotive force due to a laser pressure (the coefficient γ_p is a constant depending only on the ion species).

Modeling of the laser beam.

The laser field $\Psi = \Psi(t, \mathbf{x})$ is a solution to the following frequency wave equation (which is of Schrödinger type):

$$2i\frac{1}{c}\frac{\partial}{\partial t}\Psi + \frac{1}{k_0}\Delta\Psi + k_0(1 - N)\Psi + i\nu^\diamond\Psi = 0, \quad (31)$$

where the real coefficient ν^\diamond is related to the absorption of the laser intensity by the plasma and c the light speed.

Assume that the mean value of the plasma density is quite constant and denoted N_m , so we set:

$$N(\mathbf{x}) = N_m + \delta N(\mathbf{x}).$$

where δN is small with respect to 1. Then one can make the paraxial approximation ; that is to say the laser beam is now characterized by the space and time envelope of the electric field $\mathcal{U} = \mathcal{U}(t, \mathbf{x})$ and we set:

$$\Psi(t, \mathbf{x}) = \mathcal{U}(t, \mathbf{x})e^{ik_0\mathbf{K}\cdot\mathbf{x}}, \quad \text{where } \mathbf{K} = \sqrt{1 - N_m}\mathbf{k}.$$

Therefore, if one sets $\epsilon = \frac{1}{k_0\sqrt{1-N_m}}$, by the same procedure as mentioned in the introduction, one checks that \mathcal{U} satisfies:

$$\sqrt{1 - N_m}(i\mathbf{k}\cdot\nabla\mathcal{U} + \frac{\epsilon}{2}\Delta_{\perp}^k\mathcal{U}) + i\frac{\nu^\diamond}{2}\mathcal{U} - \frac{k_0\delta N}{2}\mathcal{U} + i\frac{1}{c}\frac{\partial\mathcal{U}}{\partial t} = 0. \quad (32)$$

It is necessary to supplement equation (32) with the same boundary condition as in the model of section 1 (and with an initial condition).

Numerical method.

We consider a mesh of finite difference type as above. The numerical treatment of the barotropic Euler system (29)(30) is a classical one, we have chosen a *Lagrange-Euler* method, see [3] for details. To deal with (32), according to the large value of the speed of light, one must perform a time implicit discretization. So at each time step, one solves firstly the Euler system with a ponderomotive force evaluated with the previous value of $|\mathcal{U}|^2$. Secondly, using the obtained values of N and of δN , one has to solve (32) ; if u^{ini} and u denote the values of the field \mathcal{U} at the beginning and the end of time step, one searches u solution to:

$$i\mathbf{k}\cdot\nabla u + i\nu u + \frac{\epsilon}{2}(\Delta_{\perp}^k u) - \mu u = \frac{i}{c\sqrt{1 - N_m}}\frac{u^{ini}}{\delta t}, \quad (33)$$

where we have set:

$$\mu = \frac{k_0\delta N}{2\sqrt{1 - N_m}}, \quad \nu = \frac{1}{c\sqrt{1 - N_m}}\frac{1}{\delta t} + \frac{1}{2\sqrt{1 - N_m}}\nu^\diamond.$$

That is exactly the equation studied in section 3, but a right hand side term has been added. So the numerical method is the same as described above ; the only modification is the adding of the right hand side term in the transport stage. Notice that the index of refraction $(1 - N)$ is equal to $(1 - 2\epsilon\mu)(1 - N_m)$. From a practical point of view, the numerical method for (32) has been implemented in a parallel way in the *HERA* platform for plasma hydrodynamics in 2D and in 3D; the parallel solver and the domain decomposition techniques are the same as the ones detailed in [3].

4.2 Numerical Results

Recall that from a practical point of view, in the transverse profile of a laser beam, one distinguishes a lot of small hot spots, called *speckles*, whose intensity is very large compared to the mean intensity of the beam. The shape of each individual speckle is a Gaussian function whose width is about a few micrometers. We present here the results of a 2D numerical simulation. One addresses a simulation box which is 600 μm long and 300 μm wide, the laser propagates with an incidence angle

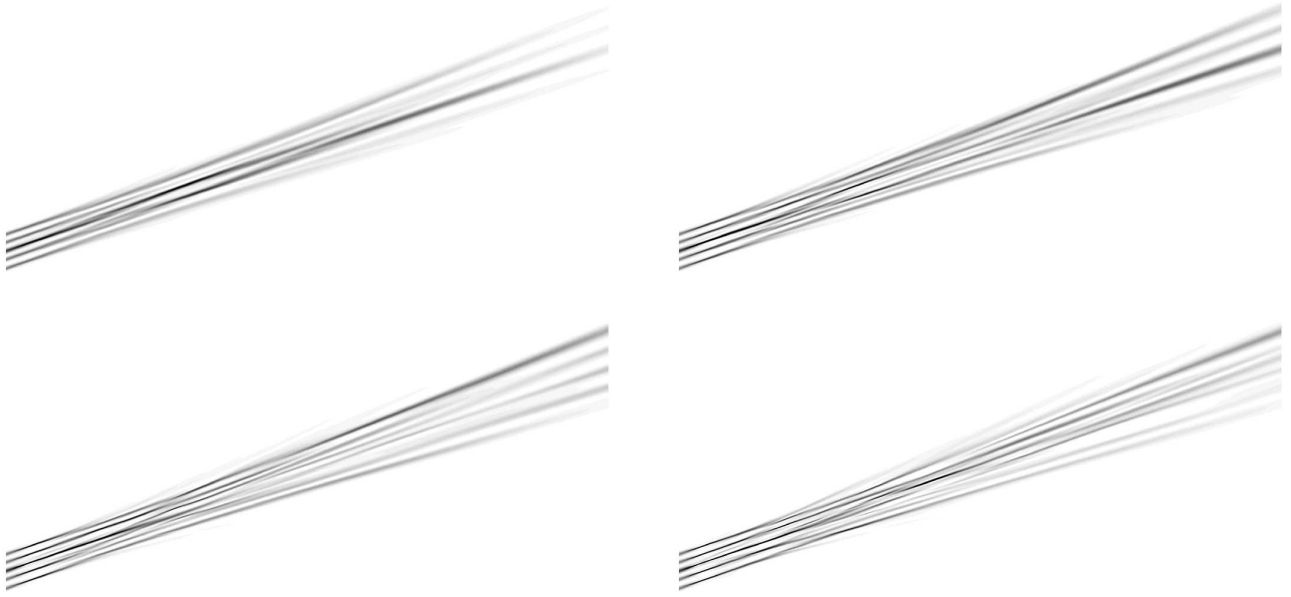


Figure 13: Snapshot of the laser intensity at the time 2.6 ps, 3.9 ps, 5.3 ps and 6.6 ps (from the top-left to the bottom-right).

of 19^0 . The incoming boundary condition $\alpha = \alpha(y)$ is independant of time and mimics a laser beam whose width is equal to $40\mu m$ with five speckles ; each speckle is modeled by a centered Gaussian function β and is characterized by a random phase ζ_k , that is to say $\alpha(y) = \sum_{k=1}^5 a_k \beta(y - Y_k) e^{i\zeta_k}$, where the α_k are random and the a_k are close to each other. The plasma has an initial density equal to $N_m = 0.15$ and the temperature is equal to $35. 10^6$ Kelvin. The mesh consists of 4 millions of cells and the time step is in the order of 0.1 picosecond (it is determined at each time step by the Courant-Friedrichs-Levy condition related to the sound speed of the plasma). The initial value of the laser intensity is zero, the plasma is progressively grabed by the ponderomotive force and on Fig.4.2, we have plotted the laser intensity at different times. One notices that the spreading of the beam at the rear side of the simulation box becomes larger when the time increases.

Conclusion

A mathematical analysis has lead to an analytical form of the solution of the tilted paraxial equation in the simple case where the refraction index and the absorption coefficients are constant. Afterwards, we proposed a numerical method for solving the initial problem which uses the previous analytical form. The scheme has the property to yield a classical scheme when incidence angle becomes zero and the equation reduces to the classical paraxial one. The numerical method is illustrated by some results on toy problems. We have also given extensions of this model, which have enlarged the capability of our plateform *HERA* for laser propagation in a plasma (see [3] and [13] for examples of simulations performed with *HERA*). This numerical method may be also extended in the case where the unit vector \mathbf{K} depends slowly on the one-dimension spatial variable $\mathbf{x} \cdot \mathbf{n}$, for

instance if one has to deal with an equation of the following type

$$i\mathbf{K} \cdot \nabla u + i\frac{1}{2}(\nabla \cdot \mathbf{K})u + \frac{1}{2k_0}\Delta_{\perp}^{\mathbf{k}}u - \mu u + i\nu u = 0, \quad \text{on } \mathcal{D}.$$

The paraxial equation in a tilted frame may be also considered in a first region where the plasma density is slowly varying with respect to the spatial variable and coupled with another model in a neighbor region where the plasma density is strongly varying: in that region the laser is no more characterized by the time-space envelope of the fast oscillating electric field but by the wave equation (31) (see [5], for results obtained in *HERA* with this model).

Appendix : Proofs for the Problem in a Quadrant

Let us first recall the definition of the square root of the differential operator $(-k_y^2 - 2i\epsilon k_x \partial_x - 2i\epsilon\nu k_x^2)$, by using the Fourier transformation, for $u \in H^{\frac{1}{2}}(\mathbb{R}_+)$:

$$\mathcal{F}_x \left(\left[\sqrt{-k_y^2 - 2i\epsilon k_x \partial_x - 2i\epsilon\nu k_x^2}(u) \right] \mathbf{1}_{x \geq 0} \right) = e^{-i\frac{\pi}{4}} \sqrt{-ik_y^2 + 2i\epsilon k_x \xi + 2i\epsilon\nu k_x^2} \mathcal{F}_x(u \mathbf{1}_{x \geq 0}).$$

For this definition to be correct, it is necessary to check that the right-hand side is the Fourier transform of a distribution which values zero in \mathbb{R}_-^* , *i.e.* it is a function h which may be extended to $\mathbb{R}^{2-} = \{a + ib, a \in \mathbb{R}, b < 0\}$ such that $\sup_{b < 0} \int_{-\infty}^{\infty} |h(a + ib)|^2 da < \infty$ (these functions are called Hardy functions). This is true if u is smooth enough. It may be checked that this definition is equivalent to the following (if $u \in H^{\frac{1}{2}+s}(\mathbb{R}_+)$ with $s > 0$):

$$\sqrt{-k_y^2 - 2i\epsilon k_x \partial_x - 2i\epsilon\nu k_x^2}(u) = \sqrt{\frac{2\epsilon k_x}{\pi}} e^{-i\frac{\pi}{4} + (i\frac{k_y^2}{2\epsilon k_x} - \nu k_x)x} \partial_x \int_0^x \frac{u(s) e^{(-i\frac{k_y^2}{2\epsilon k_x} + \nu k_x)s}}{\sqrt{x-s}} ds.$$

The aim of this appendix is to outline the proof of proposition 3 (refer to [8] for more details). If the ray enters in the quadrant (*i.e.* if $\mathbf{k} \cdot \mathbf{n} \leq 0$) our condition is a *transparent* one, and only an *absorbing* one if it goes out of it (*i.e.* if $\mathbf{k} \cdot \mathbf{n} \geq 0$).

Let U be a solution of the problem (10) (11) (17), $U \in \mathcal{C}_x^b(\mathbb{R}_+, H^{\frac{3}{2}+s}(\mathbb{R}_+))$ and V the extension of U by zero in the whole space: $V(x, y) = U(x, y) \mathbf{1}_{x \geq 0} \mathbf{1}_{y \geq 0}$. We calculate what the problem means for V , and find, using also the two boundary conditions (11) (17):

$$\begin{aligned} i\mathbf{k} \cdot \nabla V + \frac{\epsilon}{2}\Delta_{\perp} V + i\nu V &= -\epsilon k_x k_y U(0, 0) \delta_{x=0} \delta_{y=0} + \\ &\left(ik_x g \delta_{x=0} - \frac{\epsilon k_y}{2} (k_x \partial_y U|_{x=0} \delta_{x=0} - k_y U|_{x=0} \delta'_{x=0}) \right) \mathbf{1}_{y \geq 0} + \\ &\left(i\frac{k_y}{2} \left(1 - \sqrt{1 + \frac{2i\epsilon k_x}{k_y^2} \partial_x + 2i\epsilon\nu \frac{k_x^2}{k_y^2}} \right) U|_{y=0} \delta_{y=0} - \frac{\epsilon k_x}{2} (k_y \partial_x U|_{y=0} \delta_{y=0} - k_x U|_{y=0} \delta'_{y=0}) \right) \mathbf{1}_{x \geq 0}. \end{aligned} \quad (34)$$

To take the Fourier transform of this expression, we have to proceed carefully with the derivatives of U . Indeed, we can write:

$$\mathcal{F}_x((\partial_x U) \mathbf{1}_{x \geq 0}; \xi, 0) = i\xi \mathcal{F}_x(U \mathbf{1}_{x \geq 0}; \xi, 0) - U(0, 0),$$

and the equivalent formula for $\mathcal{F}_y((\partial_y U)\mathbf{1}_{y \geq 0}; 0, \eta)$. On the contrary, one directly gets:

$$\mathcal{F}_x\left(\left(\sqrt{1 + \frac{2i\epsilon k_x}{k_y^2}\partial_x + 2i\epsilon\nu\frac{k_x^2}{k_y^2}U|_{y=0}}\right)\mathbf{1}_{x \geq 0}; \xi, 0\right) = \sqrt{1 - \frac{2\epsilon k_x}{k_y^2}\xi + 2i\epsilon\nu\frac{k_x^2}{k_y^2}}\mathcal{F}_x(U|_{y=0}\mathbf{1}_{x \geq 0}).$$

We now take the Fourier transform of the formula (34). The terms depending on $U(0, 0)$ cancel one another, and we furthermore notice that:

$$i\frac{k_y}{2}\left(1 - \sqrt{1 - \frac{2\epsilon k_x}{k_y^2}\xi + 2i\epsilon\nu\frac{k_x^2}{k_y^2}}\right) - \frac{i\epsilon k_x k_y}{2}\xi = -\frac{\epsilon k_x^2}{2}A_-(i\xi).$$

Finally, using the polynomial $P_\nu(X, Y)$, we get

$$\begin{aligned} P_\nu(i\xi, i\eta)\mathcal{F}_x\mathcal{F}_y(V; \xi, \eta) = \\ \frac{\epsilon k_y^2}{2}\left(\frac{2ik_x}{\epsilon k_y^2}\mathcal{F}_y(g; \eta) - i\left(\frac{k_x}{k_y}\eta - \xi\right)\mathcal{F}_y(U\mathbf{1}_{y \geq 0}; 0, \eta)\right) + \frac{\epsilon k_x^2}{2}(i\eta - A_-(i\xi))\mathcal{F}_x(U\mathbf{1}_{x \geq 0}; \xi, 0). \end{aligned}$$

Dividing by P_ν written in one of the form (16) or (13), the equation in V reads:

$$\mathcal{F}_x\mathcal{F}_y(V; \xi, \eta) = \frac{\alpha^+(\eta)}{i\xi - R_+(i\eta)} + \frac{\alpha^-(\eta)}{i\xi - R_-(i\eta)} + \frac{\mathcal{F}_x(U\mathbf{1}_{x \geq 0}; \xi, 0)}{i\eta - A_+(i\xi)}, \quad (35)$$

where $\alpha^\pm = \pm \frac{R_\pm(i\eta) - i\frac{k_x}{k_y}\eta}{R_+(i\eta) - R_-(i\eta)}\mathcal{F}_y(U\mathbf{1}_{y \geq 0}; 0, \eta) \pm \frac{2ik_x}{\epsilon k_y^2} \frac{\mathcal{F}_y(g; \eta)}{R_+(i\eta) - R_-(i\eta)}$.

Lemma 1 *Let $s > 0$ and $U \in \mathcal{C}_x^b(\mathbb{R}_+, H_y^{\frac{3}{2}+s}(\mathbb{R}_+))$ be a function satisfying (10) (11). We suppose that $\partial_y U(x, 0) \in H_x^{-\frac{1}{2}}(\mathbb{R}_+)$ and $U(x, 0) \in H_x^{\frac{1}{2}}(\mathbb{R}_+)$. Then it verifies (17) if and only if it satisfies*

$$U(x, y)\mathbf{1}_{y \geq 0} = \mathcal{F}_y^{-1}\left(\{\hat{K}(\eta)\mathcal{F}_y(U\mathbf{1}_{y \geq 0}; 0, \eta) + \hat{G}(\eta)\}e^{R_-(i\eta)x}\right)\mathbf{1}_{y \geq 0}. \quad (36)$$

Proof. Let us take the inverse Fourier transform of the equation (35), as in the section 2.2 for the half-space problem:

$$\begin{aligned} U(x, y)\mathbf{1}_{x \geq 0}\mathbf{1}_{y \geq 0} = \mathcal{F}_y^{-1}\left(-\alpha^+(\eta)e^{R_+(i\eta)x}\mathbf{1}_{x \leq 0} + \alpha^-(\eta)e^{R_-(i\eta)x}\mathbf{1}_{x \geq 0}\right) \\ + \mathcal{F}_x^{-1}\left(-\mathcal{F}_x(U\mathbf{1}_{x \geq 0}; \xi, 0)e^{A_+(i\xi)y}\mathbf{1}_{y \leq 0}\right). \end{aligned}$$

If we multiply each side by $\mathbf{1}_{x \geq 0}\mathbf{1}_{y \geq 0}$ we obtain the formula (36). This proves that if $U \in \mathcal{C}_x^b(\mathbb{R}_+, H_y^{\frac{3}{2}+s}(\mathbb{R}_+))$ is a solution of (10) (11) (17) then it verifies the equation (36).

Conversely, let $U \in \mathcal{C}_x^b(\mathbb{R}_+, H_y^{\frac{3}{2}+s}(\mathbb{R}_+))$ be a solution of the system (10) (11)(36), such that $\partial_y U(x, 0) \in H_x^{-\frac{1}{2}}$ and $U(x, 0) \in H_x^{\frac{1}{2}}$. We carry out the same computation as precedently, and find a formula of the form:

$$\mathcal{F}_{x,y}(U; \xi, \eta) = \frac{\alpha^+(\eta)}{i\xi - R_+(i\eta)} + \frac{\alpha^-(\eta)}{i\xi - R_-(i\eta)} + \frac{\beta^+(\xi)}{i\eta - A_+(i\xi)} + \frac{\beta^-(\xi)}{i\eta - A_-(i\xi)}.$$

Taking the inverse Fourier transform and multiplying it by $\mathbb{1}_{x \geq 0} \mathbb{1}_{y \geq 0}$, we find:

$$U(x, y) \mathbb{1}_{x \geq 0} \mathbb{1}_{y \geq 0} = \mathcal{F}_y^{-1} \left(\alpha^-(\eta) e^{R_-(i\eta)x} \mathbb{1}_{x \geq 0} \right) \mathbb{1}_{y \geq 0} + \mathcal{F}_x^{-1} \left(\beta^-(\xi) e^{A_-(i\xi)y} \mathbb{1}_{y \geq 0} \right) \mathbb{1}_{x \geq 0}.$$

Since U verifies also the equation (36), we necessarily have:

$$\mathcal{F}_x^{-1} \left(\beta^-(\xi) e^{A_-(i\xi)y} \mathbb{1}_{y \geq 0} \right) \mathbb{1}_{x \geq 0} = 0 \quad \forall x > 0, y > 0.$$

The function U being continuous in y , we can take the limit when y tends to zero and obtain $\mathcal{F}_x^{-1}(\beta^-(\xi)) = 0 \quad \forall x > 0$ (confer [10] and the theory of Hardy functions).

Since β^- is the Fourier transform of a distribution null in \mathbb{R}_- , it implies that β^- is the Fourier transform of a distribution whose support is included in $\{x = 0\}$. Since $\beta^- \in L^2(\mathbb{R})$, it implies $\beta^- = 0$, which is equivalent to the Fourier transform in x of the transparent boundary condition. We have proved the lemma. \diamond

Setting $U_0(y) = U(0, y) \mathbb{1}_{y \geq 0}$, formula (36) taken at $x = 0$ reads:

$$U_0(y) = \mathcal{F}_y^{-1} \left(\hat{K}(\eta) \mathcal{F}_y(U_0; \eta) + \hat{G}(\eta) \right) \mathbb{1}_{y \geq 0}. \quad (37)$$

Thanks to lemma 1, we are able to give a meaning to the boundary condition (17) for a function $U \in \mathcal{C}_x^b(\mathbb{R}_+, L_y^2(\mathbb{R}_+))$: by definition, we say that U is solution of (10) (11) (17) *iff* it is solution of (10) (11) (36). We now prove the following lemma.

Lemma 2 *Under the assumptions of proposition 3:*

i) *the problem (10) (11) (17) admits at most one solution $U \in \mathcal{C}_x^b(\mathbb{R}_+, L_y^2(\mathbb{R}_+))$; the equation (37) admits at most one solution $U_0 \in L_y^2(\mathbb{R})$.*

ii) *The solution $u \in \mathcal{C}_x^b(\mathbb{R}_+, L_y^2(\mathbb{R}))$ to the problem (10) (11) on the half-space (with $\tilde{g} = g \mathbb{1}_{y \geq 0}$) satisfies equation (37). Moreover, $U = u|_{y > 0}$ satisfies equations (10) (11), and if $\mathbf{k}_y > \mathbf{0}$ it also satisfies equation (36).*

Proof.

i) The uniqueness of a solution of the equation (37) in $L^2(\mathbb{R})$ implies that of a solution to the equation (36) in $\mathcal{C}_x^b(\mathbb{R}_+, L_y^2(\mathbb{R}_+))$, hence of the problem (10) (11) (17). Let us take $g = 0$ and suppose that a function $U_0 \in L^2(\mathbb{R})$ verifies:

$$U_0(y) = \mathcal{F}_y^{-1} \left(\hat{K}(\eta) \mathcal{F}_y(U_0; \eta) \right) \mathbb{1}_{y \geq 0}.$$

Let $V_0(y) = \mathcal{F}_y^{-1} \left(\hat{K}(\eta) \mathcal{F}_y(U_0; \eta) \right)(y)$. The function V_0 verifies the following equation, because $U_0 = V_0 \mathbb{1}_{y \geq 0}$:

$$V_0(y) = \mathcal{F}_y^{-1} \left(\hat{K}(\eta) \mathcal{F}_y(V_0 \mathbb{1}_{y \geq 0}; \eta) \right) = \int_0^\infty K(y-s) V_0(s) ds.$$

We separate V_0 into $V_+ = V_0 \mathbb{1}_{y \geq 0}$ and $V_- = V_0 \mathbb{1}_{y < 0}$. Since $V_0 \in L^2(\mathbb{R})$, $V_\pm \in L^2(\mathbb{R}_\pm)$, *i.e.* the functions $\hat{V}_\pm := \mathcal{F}_y(V_\pm; \eta)$ belong to the Hardy spaces $H^{2\pm}$. The resulting equation writes:

$$\hat{V}_+(\eta) (1 - \hat{K}(\eta)) = \frac{1}{2} \left(1 + \frac{1}{\sqrt{1 - \frac{2\epsilon k_y}{k_x^2} \eta + 2i\nu \epsilon \frac{k_y^2}{k_x^2}}} \right) \hat{V}_+(\eta) = -\hat{V}_-(\eta).$$

The idea of the proof is to find an H^{2-} function on the left side, equal to a H^{2+} function on the right side: since $H^{2+} \cap H^{2-} = 0$, it will imply that both sides are null. We use the fact that the function $\frac{1}{\sqrt{1 - \frac{2\epsilon k_y}{k_x^2}\eta + 2i\nu\epsilon\frac{k_y^2}{k_x^2}}}$ can be extended analytically by a uniformly bounded function, respectively: in $\mathbb{R}^{2-} = \{\eta - i\lambda, \lambda > 0\}$ if $k_y > 0$, and in \mathbb{R}^{2+} if $k_y < 0$.

ii) Let $u \in \mathcal{C}_x^b(\mathbb{R}_+, L_y^2(\mathbb{R}))$ be the solution of the problem (10) (11) in the half-space, with an entrance boundary condition equal to $\tilde{g} \in H^{-\frac{1}{2}}(\mathbb{R})$. We have seen that u verifies $u(x, y)\mathbb{1}_{y \geq 0} = \mathcal{F}_y^{-1}\left(\alpha_{1/2}^-(\eta)e^{R_-(i\eta)x}\right)\mathbb{1}_{y \geq 0}$,

$$\text{with } \alpha_{1/2}^-(\eta) = \hat{K}(\eta)\mathcal{F}_y(u; 0, \eta) + \hat{G}(\eta).$$

This is almost equation (36): we have $\alpha^- = \alpha_{1/2}^- - \hat{K}\mathcal{F}_y(u\mathbb{1}_{y \leq 0}; 0, \eta)$.

Let us distinguish the two cases, according to the sign of k_y .

1. $k_y > 0$

We have seen in section 2.2 that u verifies $\mathcal{F}_y(u; 0, \eta) = \frac{2\mathcal{F}_y(g\mathbb{1}_{y > 0}; \eta)}{1 + \sqrt{1 - \frac{2\epsilon k_y}{k_x^2}\eta + 2i\nu\epsilon\frac{k_y^2}{k_x^2}}}$.

Since the function $\frac{1}{1 + \sqrt{1 - \frac{2\epsilon k_y}{k_x^2}\eta + 2i\nu\epsilon\frac{k_y^2}{k_x^2}}}$ can be extended analytically by a uniformly bounded function in \mathbb{R}^{2-} , if $g \in L^2(\mathbb{R}_+)$ then $\mathcal{F}_y(u; 0, \eta) \in H^{2-}$, so $u(0, y) = u(0, y)\mathbb{1}_{y \geq 0}$. This shows that in this case, $\alpha^- = \alpha_{1/2}^-$ so u verifies the equation (36).

2. $k_y < 0$

Let us write $\alpha_{1/2}^-(\eta) = \alpha^-(\eta) + \hat{K}(\eta)\mathcal{F}_y(u\mathbb{1}_{y \leq 0}; 0, \eta)$, with the preceding definition of α^- . Since $u(0, \cdot) \in L^2(\mathbb{R})$, $\hat{K}(\eta)\mathcal{F}_y(u\mathbb{1}_{y \leq 0}; 0, \eta) \in H^{2+}$. The function u verifies the following equation:

$$u(0, y)\mathbb{1}_{y \geq 0} = \mathcal{F}_y^{-1}(\alpha^-(\eta))\mathbb{1}_{y \geq 0} + \mathcal{F}_y^{-1}(\hat{K}(\eta)\mathcal{F}_y(u\mathbb{1}_{y \leq 0}; 0, \eta))\mathbb{1}_{y \geq 0}.$$

Since $\hat{K}(\eta)\mathcal{F}_y(u\mathbb{1}_{y \leq 0}; 0, \eta) \in H^{2+}$, it is the Fourier transform of a function null in \mathbb{R}_+ , so the last member of the equation values zero. This shows that $u(0, y)$ verifies the equation (37).

◇

We deduce the proposition 3 and its assertion *i*) from this lemma (see [8] for more details).

To prove the assertion *ii*) of theorem 3, let us assume that $k_y < 0$ and denote by u the solution of the half-space problem and by U that in the quadrant. we obtain easily the following relation :

$$(u - U)\mathbb{1}_{y \geq 0} = \mathcal{F}_y^{-1}\left(e^{R_-(i\eta)x}\hat{K}(\eta)\mathcal{F}_y(u\mathbb{1}_{y \leq 0}; 0, \eta)\right)\mathbb{1}_{y \geq 0}. \quad (38)$$

Let us now assume that $g(y) = h(y - A)$, $A > 0$, $h \in H^{-\frac{1}{2}}(\mathbb{R})$ and $Supp(h) \subset \mathbb{R}_+^*$. We can write:

$$\mathcal{F}_y(u_0; \eta) = \frac{\mathcal{F}_y(h; \eta)e^{-i\eta A}}{1 + \sqrt{1 - 2\epsilon\frac{k_y}{k_x^2}\eta + 2i\nu\epsilon\frac{k_y^2}{k_x^2}}} = \mathcal{F}_y(H; \eta)e^{-i\eta A},$$

with a function $H \in L^2(\mathbb{R})$. We then have $u_0 = H(y - A)$, so $\|u_0\mathbb{1}_{y \leq 0}\|_{L^2} = \|H|_{y \leq -A}\|_{L^2}$ tends to 0 when $A \rightarrow +\infty$. We use the relation (38) to estimate the difference between the half-space and the quarter plane solutions, since $\mathcal{R}e(R_-(i\eta)) < 0$:

$$\|(u - U)(x, y)\mathbb{1}_{y \geq 0}\|_{L_x^\infty(\mathbb{R}_+, L_y^2(\mathbb{R}))} \leq \|\hat{K}\mathcal{F}_y(u_0\mathbb{1}_{y \leq 0})\|_{L^2(\mathbb{R})} \leq C\|H|_{y \leq -A}\|_{L_y^2(\mathbb{R})}.$$

References

- [1] A. Arnold, *Numerically Absorbing Boundary Conditions for Quantum Evolution Equations*, VLSI Design **6** No. 1-4 p. 313-319, (1998).
- [2] J.P. Bérenger, *A Perfectly Matched Layer*, J. Comp. Physics **114**, p. 185-200 (1994).
- [3] Ph. Ballereau, M. Casanova, F. Duboc *et al.* *Simulation of the Paraxial Laser Propagation coupled with Hydrodynamics in 3D Geometry*, J. Scientific Comp. **33**, p.1-24, (2007).
- [4] R.L. Berger, B.F. Lasinski *et al.*, *Theory and three-dimensional Simulation of Light Filamentation*, Phys. Fluids B, **5**, p. 2243-2258 (1993).
- [5] S. Desroziers, F. Nataf, R. Sentis, *Simulation of Laser Propagation in a plasma with a Frequency Wave Equation*, J. Comp. Physics, to be published (2007).
- [6] L. Di Menza, *Transparent and Absorbing Boundary Conditions for Schrödinger Equations*, Num. Funct. Anal. Optimization, **18**, p 759 (1997).
- [7] J. D. Lindl *et al.*, *The physics basis for ignition using indirect-drive target (§III)*, Phys. Plasmas, **11**, pp. 339-491 (2004)
- [8] M. Doumic, *Etude asymptotique et simulation numérique de la propagation laser en milieu inhomogène*, Ph. D. Dissertation, University Paris VII, (2005).
- [9] M. R. Dorr, Garaizar F. X., Hittinger J. A., *Simulation of laser-Plasma filamentation*, J. Comp. Phys., **177**, p.233-263 (2002).
- [10] H. Dym, H.P. McKean, *Fourier Series and Integrals*, Academic Press, (1972).
- [11] M. Ehrhardt, A. Arnold, *Discrete Transparent Boundary Conditions for Schrödinger Equations*, Riv. Mat. Univ. Parma, **6**, p. 57 (2001).
- [12] M.D. Feit, J.A. Fleck, *Beam non paraxiality*, J. Opt.Soc.Am. B, **5** , p633-640 (1988).
- [13] P. Loiseau *et al* *Laser beam smoothing induced by simulated Brillouin scattering*, Phys. Rev. Letters, **97**, p.205001 (2006).
- [14] R. Hadley, *Transparent Boundary Condition for the Beam Propagation Method*, IEEE, J. Quantum Electronics, **28**, p.363 (1992).
- [15] D. Lee, A. D. Pierce, E.-S. Shang, *Parabolic Equation Development in the twentieth century*, J. Comput. Acoust., **8** (2000), p.527-637.
- [16] R. J. LeVeque, *Numerical Methods for Conservation Laws*, Birkhauser-Verlag, Basel, 1990.
- [17] R. Sentis, *Mathematical models for laser-plasma interaction*, ESAIM-Mathematical Modelling and Numerical Analysis, **39**, p. 275-318 (2005).

- [18] H.A. Rose, *Laser beam deflection*, Phys. Plasmas, **3**, p. 1709-1727 (1996).
- [19] V.T. Tikhonchuk, a.a. Zozulya, *Structure of Light beams in self-pumped four wave mixing geometries*, Prog.Quant. Electr., **15**, p.231 (1992).
- [20] F. Walraet, G. Riazuelo, G. Bonnaud, *Propagation in a plasma of a smooth Laser Beam*, Phys. Plasmas, **10**, p. 811-919 (2003).